Journal of Rehabilitation in Civil Engineering 8-3 (2020) 60-71

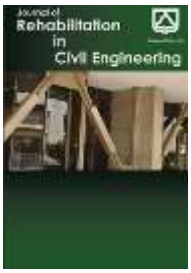

journal homepage: http://civiljournal.semnan.ac.ir/

Effect of Deformed and Plain Rebars on the Behavior of Lightly Reinforced Boundary Elements

M.A. Pourakbar [1] and S. Tariverdilo [1*]
1. Department of Civil Engineering, Faculty of Engineering, Urmia University, Urmia, Iran.

Corresponding author: *s.tariverdilo@urmia.ac.ir*

ARTICLE INFO

Article history:
Received: 14 February 2020
Accepted: 06 April 2020

Keywords:
Boundary element,
Plain rebar,
Deformed rebar,
Rebar fracture,
Out of plane buckling.

ABSTRACT

In recent earthquakes common failure modes of lightly reinforced shear walls includes rebar fracture and out of plane buckling of boundary elements. In latest edition of ACI 318 and also latest amendment of NZS 3101-2006 to avoid rebar fracture in boundary elements, minimum longitudinal reinforcement ratio is increased. This experimental study investigates that rather than increasing the reinforcement ratio, is it possible to avoid rebar fracture by use of plain rebars in the critical sections of boundary elements in lightly reinforced shear walls. Experimental program includes specimens with plain and deformed rebars tested under monotonic and cyclic loading. Strain profile of the rebars are evaluated employing correlation between hardness and residual strain. Results indicate that failure of specimens with plain rebars occurs on single crack, however they have more uniform strain profile. On the other hand, in the specimens with plain and deformed rebars, out of plane buckling occurs at same crack width, but different elongations. It is shown that local strain demand (crack width) has better correlation with out of plane buckling in comparison with average axial strain.

1. Introduction

Low ratio of longitudinal rebars in lightly reinforced shear/bearing walls could leads to limited cracking and large tensile strain in the longitudinal rebars at crack locations. This could cause fracture of rebar even in relatively small drifts. This type of failure was observed in boundary elements (BE) of several shear walls in 1985 Chile earthquake and latter in 2010/2011 Canterbury earthquakes, resulting in collapse of a number buildings [1].

One of the reasons for imposing minimum reinforcement requirement for beams and columns in the building codes (e.g. ACI 318-19) is to provide a minimum ratio of flexural strength (controlled by longitudinal rebar's

DOI: 10.22075/JRCE.2020.19767.1381

strength and ratio) to cracking strength (controlled by concrete strength and sectional dimensions) [2]. This requirement indirectly guarantees distribution of nonlinear deformation in relatively large length and occurrence of secondary cracks [3]. While this concept is applied on beams and columns, this is not the case for shear walls. Use of smaller ratio of reinforcements for longitudinal rebars in the shear walls (about 0.0025) is main reason for localization of nonlinear deformation in single crack and subsequent fracture of the longitudinal rebars in BE of lightly reinforced shear walls.

Loading history could have significant impact on the seismic response of BEs. Moehle and coworkers investigated ductility of BEs subjected to monotonic compression loading [4]. Massone et al. examined effect of tensile excursion on the compression failure of boundary elements with noncompliant detailing [5]. In addition to compression failure controlled by concrete spalling, other common modes of failure in lightly reinforced shear walls subjected to large tensile excursion are rebar fracture and out of plane buckling (OOPB) of BEs [6].

Concentrating on the failure of lightly reinforced shear walls, several numerical and experimental investigations are carried out by different researchers including Hoult et al. [7] , Lu et al. [8]. Comparing seismic response of walls with different ratio of longitudinal rebars, they found the need for substantial increase in the code's prescribed minimum reinforcement to avoid strain localization in the longitudinal rebar. These findings lead to changes in the third amendment of NZS 3101-2006 [9] and also ACI 318-19. It should be noted that the proposed increase in the ratio of longitudinal rebars in NZS 3101-2006 applies on web and BE of shear wall, while ACI 318-19 only requires increase in BE reinforcement ratio.

As found by Paulay and Preistley [10] tensile strain of longitudinal rebars controls out of plane buckling (OOPB) of BE. Rosso et al. [11] investigated the effect of cyclic loading on OOPB of thin BE with single layer of reinforcement. They found that for BE with larger ratio of longitudinal rebars, the element is more prone to out of plane buckling. Increase in the rebar ratio increases the number of cracks and at the same time increases the possibility of OOPB. Haro et al. investigated OOPB of well confined BEs subjected to different loading protocols [12]. They found that in addition to the ratio of longitudinal rebars, the lateral drift demand is also detrimental in the initiation of OOPB.

While control of strain localization in rebars requires higher ratio of longitudinal rebars, increase in this ratio makes the BE more susceptible to OOPB [11]. This contradictory effect of the ratio of longitudinal rebars on strain localization and OOPB, means that increase in reinforcement ratio should be accompanied with larger section dimension to avoid OOPB.

While debonding is extensively used in prestressed concrete structures, it was only recently that its use become common in the reinforced concrete structures. It was shown by Kawashima et al [13], Mashal et al. [14], and Nikoukalam and Sideris [15] that it is possible to increase drift capacity of columns by debonding rebars in the plastic hinge zone. Patel et al. decreasing rib height of deformed rebars tried to investigate the effect of rebar debonding on its strain profile [16]. While rib height and spacing for standard D12 rebar are 1.2 and 8.5 mm, for reduced rib height rebar these dimensions are 0.6 and

8.5 mm, respectively. They concluded that decreasing rib height reduces the number of cracks and is accompanied by increase in the crack width and strain penetration depth.

This paper investigates the effect of using deformed and plain rebars on the strain localization of longitudinal rebars and also OOPB of BE of lightly reinforced shear walls. Plain rebars could be spliced at the critical section of wall using welding or mechanical coupler to reduce strain localization in the location of possible single cracking. Specimens are designed to replicate boundary elements of lightly reinforced shear walls. Monotonic and cyclic tests are carried out to study cracking pattern, reinforcement strain profile and cracking induced instability in boundary elements as affected by the use of deformed and plain rebars in the nonlinear deformation zone of BE.

2. Measures Used to Evaluate Test Results

Accuracy in the evaluation of the rebar axial strain is essential in the analysis of vulnerability to out of plane buckling (OOPB) of BEs and rebar fracture.

Deformation in elements that undergoes large nonlinear displacements could be decomposed in two components, a) deformation along the element length, b) deformation due to rebar elongation in the element foundation. A commonly used estimate of effective plastic hinge length (l_p) for flexural elements as proposed by Paulay and Priestley is

$$l_p = 0.08l + 0.022 f_y d_b \quad (1)$$

where l is element length from point of zero to maximum moment, f_y and d_b are rebar yield stress and diameter. For plastic curvature of φ_p, the resulting plastic rotation (θ_p) could decomposed into two components as follows

$$\theta_p = \varphi_p l_p = 0.08 l \varphi_p + 0.022 f_y d_b \varphi_p = \theta_{p1} + \theta_{p2} \quad (2)$$

The first term gives the plastic rotation due to plastic deformation along the element length and the second term gives plastic rotation due to strain penetration (rebar elongation in the foundation) .

Strain penetration into foundation could make significant contribution to specimen elongation and should be reduced from total elongation to reach axial strain that is effective in OOPB. Another approximation for strain penetration length proposed by Priestley and Park [17] is

$$l_{sp1} = 6 d_b \quad (3)$$

Also accounting for concrete compression strength $f_c^{'}$, Berry et al. proposed following equation for strain penetration [18]:

$$l_{sp2} = 0.1 \frac{d_b f_y}{\sqrt{f_c^{'}}} \quad (4)$$

After test termination and having the tested rebars, it is only possible to evaluate average strain in the rebar length. This will not be helpful to drive strain profile along the element length specially at the locations of cracks, where the reinforcements vulnerable to fracture. On the other hand, using strain gage it is only possible to drive the local strain at the strain gage location, but there is no guarantee that cracks occur at the location of installed strain gage.

There are good progress in damage identification techniques involving damage detection, localization and assessment [19-22]. This techniques provide a good device for interpreting results of ultrasonic and

acoustic nondestructive tests. Apart from damage identification techniques, there are two common ways to drive the strain profile in a length rather than at a point, a) using optical fiber with distributed reflector installed in the fiber core (e.g. [23]), b) employing correlation of hardness and strain to drive strain profile by evaluating hardness of tested rebar. While the former method is more accurate, it is expansive. The latter one is much cheaper, although is less accurate.

To evaluate strain profile along the specimen length, this study employs well known correlation between hardness and strain for metals [24]. There are different types of hardness tests, including Brinell, Vikers and Rockwell tests. Rockwell B hardness test is carried out using indent universal hardness test machine on rebars. Different types of Rockwell tests are suitable for different material types. Various Rockwell test types employ different applied load and different indenter shape and size. Rockwell B hardness test is done using applied load of 1000 N with spherical steel indenter of 1.6 mm in diameter. Tensile tests are interrupted at different residual strains to drive correlation between hardness and strain. Fig. 1 shows the test results for establishing correlation between residual strains and Rockwell hardness. After completion of test on specimens, again hardness test is done along the rebar length and using established correlation between hardness and strain, it will be possible to drive strain profile for rebar.

Extensive tensile cracking of boundary elements could lead to out of plane instability of BE. Paulay and Preistley found that out of plane buckling depends on normalized out of plane displacement [10].

$$\xi = \frac{w_{\text{out of plane}}}{b} \le 0.5\left(1 + 2.35\frac{\rho f_y}{f_c'} - \sqrt{5.53\left(\frac{\rho f_y}{f_c'}\right)^2 + 4.70\frac{\rho f_y}{f_c'}}\right) \quad (5)$$

where average critical strain corresponding to OOPB for one layer of reinforcement will be:

$$\varepsilon_{cr} = 4\left(\frac{b}{l_o}\right)^2 \xi_{cr} \quad (6)$$

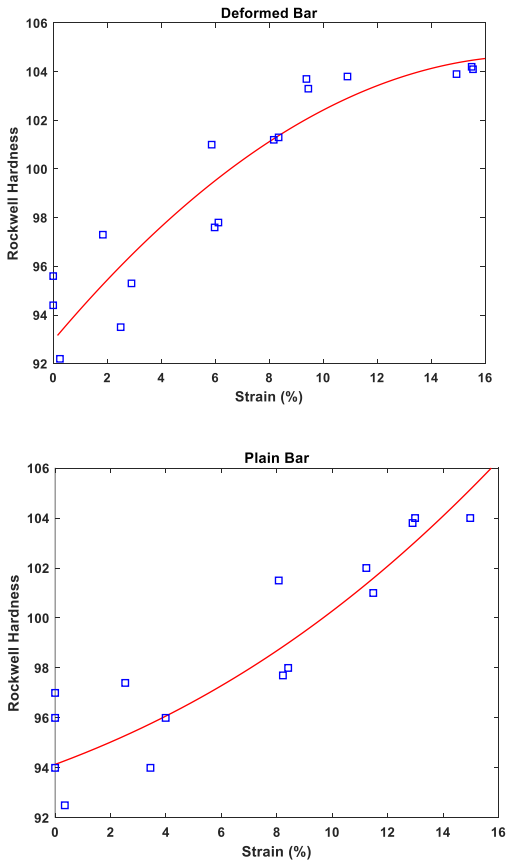

Fig. 1. Rockwell hardness versus residual strain and graph depicting result of regression analysis (a) deformed rebars (b) plain rebars.

3. Experimental Program

Compared with beams and columns, moment gradient along shear wall height is much smaller and there is nearly uniform axial loading on BE near critical section of shear wall [16]. This justifies using specimen under uniaxial loading to study boundary element of shear walls, which is also adopted by other

researchers including Rosso et al. [11] and Haro et al. [12].

Experimental program includes two monotonic and four cyclic tests with deformed and plain longitudinal rebars (Table 1). Tests are conducted using 1000 kN capacity universal jack of center for infrastructure research at Urmia University. Table 1 gives description of samples considered in the study and Fig. 2 depicts the test setup and instrumentation. LVDTs are used to monitor axial deformation and lateral deformation at the initiation of out of plane buckling, is measured using gages along the element length.

Table 1. Samples description, geometry and reinforcement.

Sample Designation	Descrption	Dim. (mm) *width1*x *widht2*x *length*	Long. Bar	Rein. Ratio (%)	Trans. Rein.
BM2	Deformed Rebar Monotonic loading	150x150x 1000	T10	0. 347	T6@70
BC1	Deformed Rebar Cyclic loading	"	T10	0. 347	T6@70
BC2	Deformed Rebar Cyclic loading	"	T10	0. 347	T6@70
PM1	Plain Rebar Monotonic loading	"	T10	0. 347	T6@70
PC1	Plain Rebar Cyclic loading	"	T10	0. 347	T6@70
PC2	Plain Rebar Cyclic loading	"	T10	0. 347	T6@70

Following Hilson et al. and Rosso et al., an asymmetric loading protocol is adopted for cyclic loading [25,11]. The loading protocol is symmetric until reaching compression strain of 0.003, then protocol becomes asymmetric, where maximum compression strain remains constant and meanwhile maximum tensile strain increases (Fig. 3).

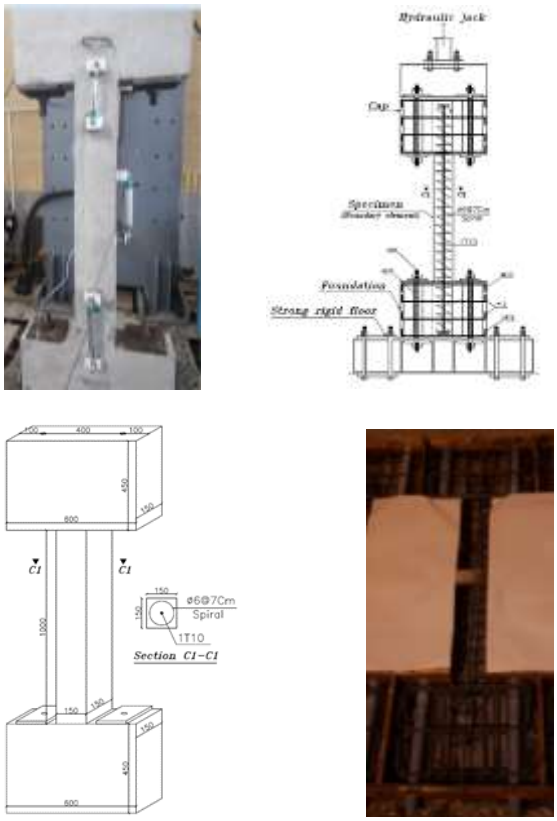

Fig. 2. Specimen's setup and instrumentation.

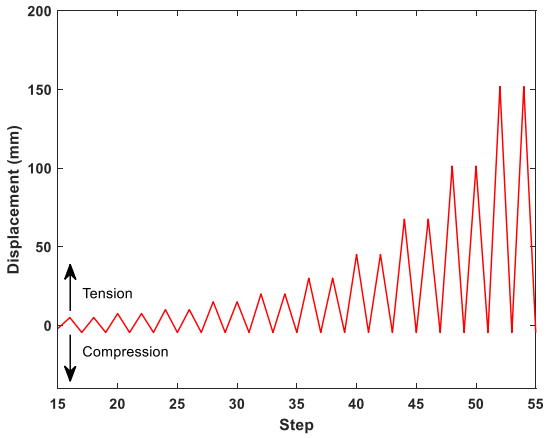

Fig. 3. Loading protocol used in the experiments.

Material properties for deformed and plain rebars and concrete are given in Table 2. Fig. 4 shows stress-strain diagram of the rebars obtained under uniaxial tensile loading.

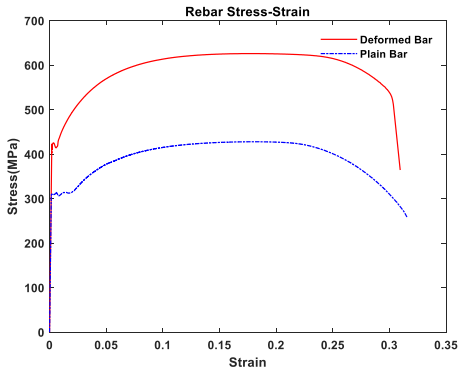

(a)

(b)

(c)

Fig. 4. Deformed and plain rebars, a) stress-strain diagram, b) fractured plain rebar, c) fractured deformed rebar.

Table 2. Material properties for concrete and reinforcements.

Designation	Material Property	Reinforcements	
		Deformed	Plain
f_y	Yield Stress (MPa)	433	307
f_{su}	Ultimate Strength (MPa)	622	427
ε_{fc_test}	Fracture Elongation strain in $5d_b$	0.30	0.31
	Fracture Elongation strain in $10d_b$	0.27	0.25
	Fracture Elongation strain in 200 mm	0.21	0.23
	Material Property	**Concrete**	
$f_c^{'}$	28 days strength (MPa)	30	

4. Monotonic Tests

Monotonic tests on BE include one test on deformed rebar and another one on plain rebar. Fig. 5a shows load-deflection and Fig. 5b gives the cracking pattern of the specimens. The cracking sequence and width are given in Table 3. For specimen with deformed rebar, fracture has occurred in crack at element-foundation interface, while for specimen with plain rebars there is a single crack within element length.

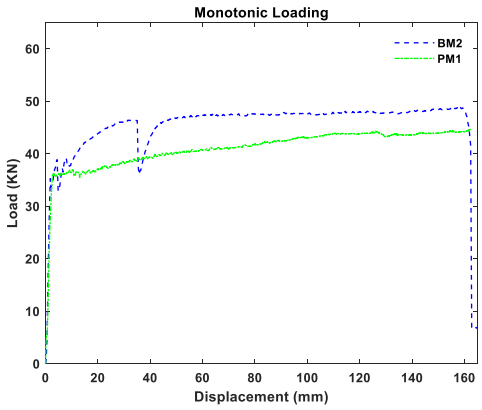

(a)

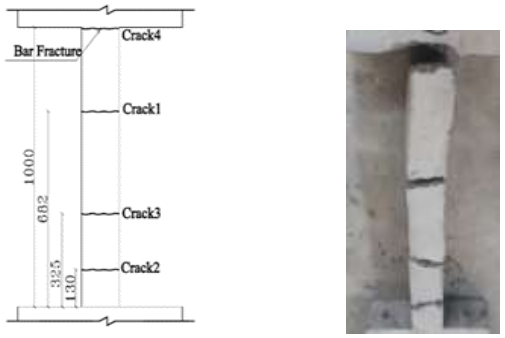

(b)

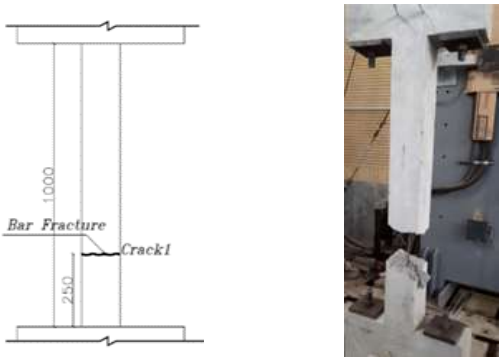

(c)

Fig. 5. Test results for specimens under monotonic loading, a) load-deflection, b) deformed rebar cracking pattern, c) plain rebar cracking pattern.

After test completion, hardness evaluation is done on the specimen rebar and then using correlations established between hardness and strain (Fig. 1), strain along the rebar length is back calculated. In assessing results of this strain profile, it should be noted that this method can not capture accurately strain profile near rebar fracture zone. This means that it is only useful for deriving strain profile at tensile loads smaller than tensile strength, which is also useful range of rebar nonlinear deformation. Fig. 6 gives evolution of hardness and axial strain of the specimens BM2 and PM1 along deformed length, which is slightly larger than undeformed length (1000 mm).

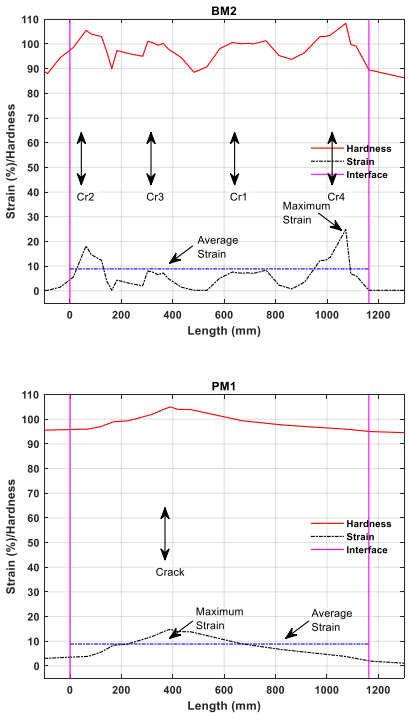

Fig. 6. Evolution of Rockwell hardness and axial strain (back calculated from hardness values) with length for specimens under monotonic loading.

As could be seen, there is good correlation between strain peaks and crack locations. Due to tension stiffening, rebar strain between cracks in specimen BM2 reduces to nearly zero. In specimen PM1, minimum strains are located at element-foundation interface, contrary to that for the specimen with deformed rebars, where fracture and maximum strain are found at the interface. Maximum strain and ratio of maximum strain to average strain for BM2 are 0.25 and 4.0, and for PM1 are 0.15 and 1.8. This is a clear indication of large susceptibility of bonded specimens to strain localization and that more uniform strain distribution for specimen with plain rebar is anticipated in nonlinear deformation zone.

Strain profile could also be used to evaluate strain penetration into foundation and strain penetration length (l_{sp}) on either sides of intermediate cracks. Strain penetration into foundation is important for improving accuracy in the evaluation of average axial deformation of the element. On the other hand, strain penetration length on either side of crack could be used to find maximum available strain capacity of the rebar between cracks.

For deformed rebar and considering strain evolution along the element length in Fig. 5, strain penetration length (length at which rebar strain reduces to zero) could be evaluated to be $12d_b$. Altheeb et al. developed an experimental program to derive strain profile of rebar in the vicinity of crack in a notched specimen simulating BE of lightly reinforced shear wall [26]. Their result shows that strain penetration length is at least $9d_b$. At the same time, Patel et al., again considering BE of lightly reinforced shear walls, concluded that this length could be approximated to be equal to $3.6d_b$ for yield stress of about 300 MPa [16]. Patel et al. also found that for rebars with reduced rib height (half of standard deformed rebars) this length increases to $8d_b$ [16]. For plain rebars, as

could be inferred from Fig. 5, strain penetration length is much larger and noting that increase in rebar length decreases the fracture elongation strain (see Table 1), this explains why axial elongation strain for specimen with plain rebars is not larger than that for specimen with deformed rebars.

In Table 3 different estimates of strain penetration are compared for different specimens. As discussed earlier, it is important to have an accurate estimation of the rebars strain on the onset of OOPB and rebar fracture. In this study different estimates of rebar strain are evaluated as follows:

1) Ignoring strain penetration and dividing total elongation (Δ_t) by elements length (l) giving ε_{sm1}.

2)Using correlation of hardness-strain to obtaining strain of the rebar after test completion, ε_{sm2} (only applicable for specimens under monotonic loading).

Table 3. Evaluation of average and local strain for specimens under monotonic loading.

Sample Designation		BM2	PM1
Crack Sequence and Width (mm)	1	20	163*
	2	17	-
	3	35	-
	4	91*	-
Total Elong.		163	163
Average Strain (ε_{sm1})		0.163	0.163
Local Strain (ε_{sm2}) At Each Crack	1	0.08	0.15
	2	0.18	-
	3	0.08	-
	4	0.25	-

* Rebar fracture crack

Accuracy of strain estimate will be instrumental in predicting axial strain triggering out of plane buckling of BE. In fact review of Fig. 5 unveils that the extent of strain penetration is much smaller than that could be predicted using Eq. (3) to Eq. (4). The order of error in estimating local strain (ε_{sm2}) from average total strain (ε_{sm1}) could be as large as 60 percent. This should be considered in any evaluation of rebars fracture.

5. Specimens under Cyclic Loading

Two specimens with deformed rebars (BC1 and BC2) and two specimens with plain rebars (PC1 and PC2) are tested under cyclic loading. Fig. 7 and Fig. 8 give the load-displacement and cracking pattern of the specimens. Also shown in Fig. 7 is the onset of out of plane buckling for the specimens, which is depicted by asterisk.

While in the specimens with deformed rebars (BC1 and BC2) there is extensive cracking with at least 4 distinct cracks, in both of the specimens with plain rebars (PC1 and PC2) there is single crack. Consequently at same axial displacement the cracks width in for PC1 and PC2 is much larger than that for BC1 and BC2 (see Table 4).

Table 4. Evaluation of strain for specimens under cyclic loading.

Sample Designation	Status	Crack Number and Width (mm)						Total Elong.	Aver. Strain ε_{sm1}
		1	2	3	4	5	6		
BC1	OOPB	5	4	9**	7	7	-	32	0.032
	Test End	20	19	14*	21	25	12	111	0.111
BC2	OOPB	10**	5	9	8	-	-	32	0.032
	Test End	25	19*	22	18	-	-	84	0.084
PC1	OOPB	8**	-	-	-	-	-	8	0.008
	Test End	48*	-	-	-	-	-	48	0.048
PC2	OOPB	7**	-	-	-	-	-	7	0.007
	Test End	48*	-	-	-	-	-	48	0.048

* Rebar fracture crack

** Maximum crack width initiating out of plane buckling

For both cases of deformed and plain rebars, OOPB have been occurred at approximately same crack width (8~10 mm). This could indicate that local strain demand (crack width) has better correlation with OOPB than average strain demand. Referring to Table 3, while local strain in the specimens with plain rebars could be approximated by total elongation (i.e. $\varepsilon_{sm2} \approx \varepsilon_{sm1}$), in the specimens with deformed rebars, local strain could be much larger (i.e. $\varepsilon_{sm2} > \varepsilon_{sm1}$). However, knowing approximate crack spacing, it is possible to calculate the crack width corresponding to OOPB.

Occurrence of OOPB in specimens with deformed rebars or plain rebars at same crack width suggests that it would be better to correlate onset of OOPB to crack width rather than axial strain. Fig. 9 compares correlation between axial strain vs length/width and crackwidth/d_b vs length/width for different samples. As could be seen crack width compared to average axial strain has much better correlation with OOPB.

For elements with larger ratio of longitudinal reinforcement, number of cracks increases and at the same time difference between strain calculated from total strain (ε_{sm1}) and local strain (ε_{sm2}) that controls crack width decreases. This explains why in elements with large reinforcement ratio, good correlation between Eq. (6) and average axial strain is reported [12].

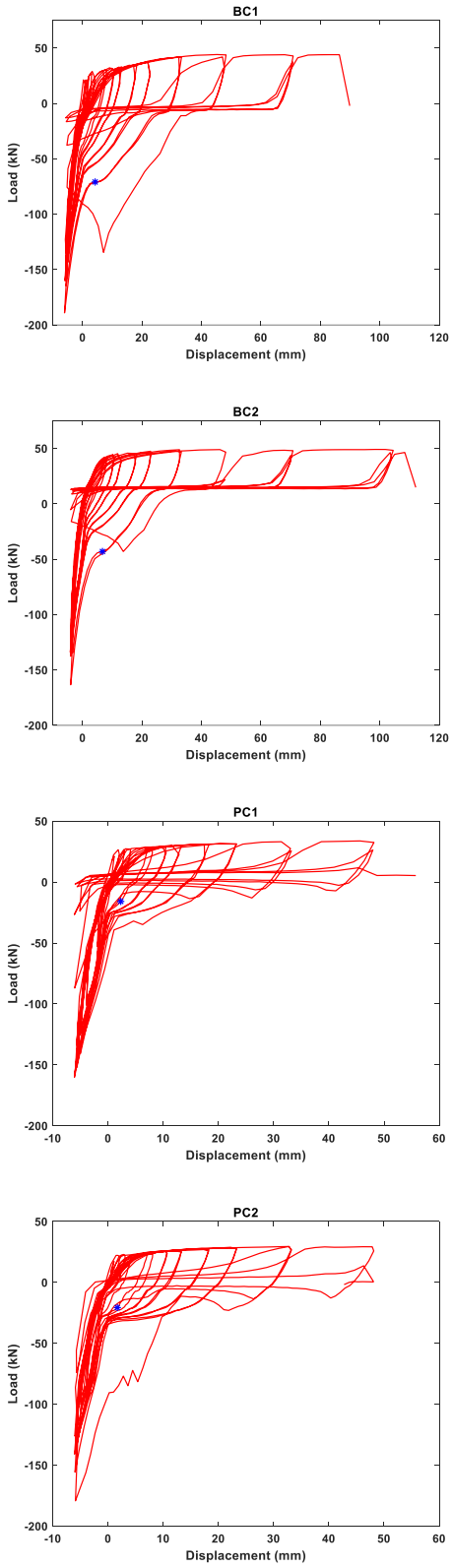

Fig. 7. Load-displacement for specimens under cyclic loading.

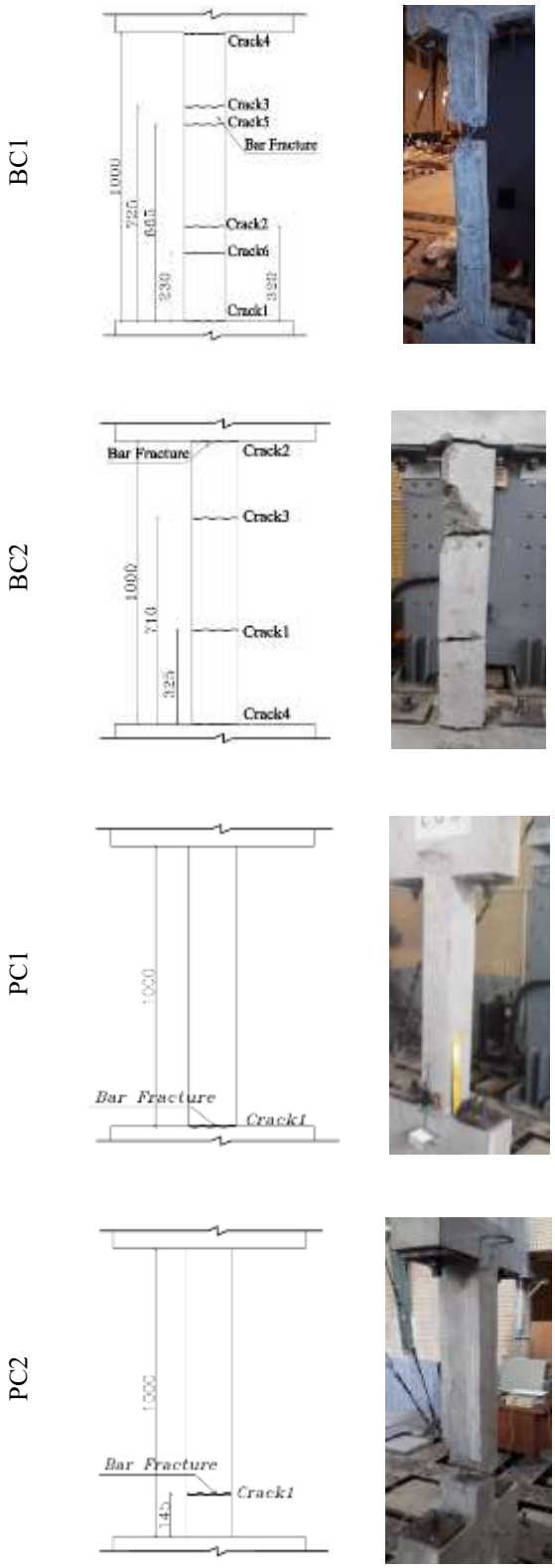

Fig. 8. Cracking pattern for specimens under cyclic loading.

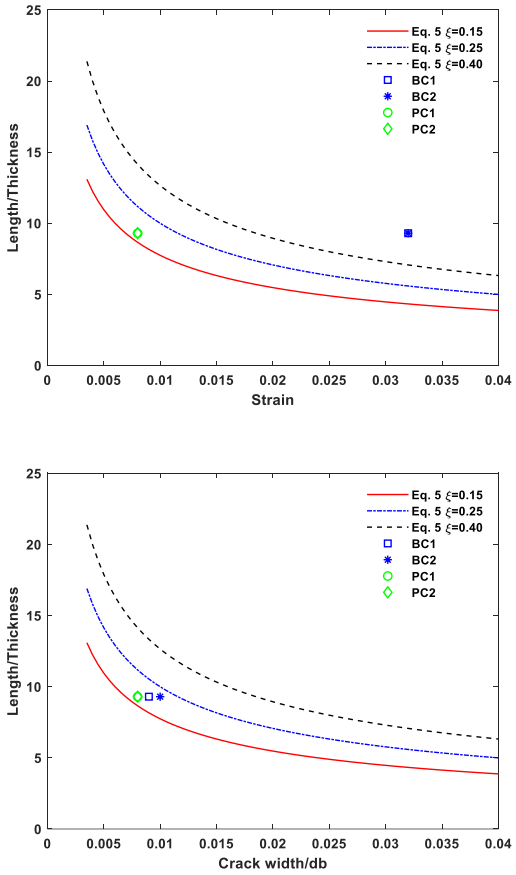

Fig. 9. Correlation between rebar tensile strain or crack width/d_b and slenderness ratio of the specimens.

6. Conclusion

Effect of use of plain rather than deformed rebars, in boundary elements of lightly reinforced shear walls, on the strain profile and out of plane buckling of boundary elements is investigated experimentally. Experimental program includes monotonic and asymmetric cyclic loadings. Correlation between hardness and strain is employed to derive strain profile at the end of tests. While previous works relates out of plane buckling (OOPB) with average tensile strain of the longitudinal rebars, it is shown that for boundary elements of lightly reinforced shear walls, maximum crack width has better correlation with OOPB. For plain and

deformed rebars OOPB occurs at approximately same maximum crack width. However results necessitates further researches to evaluate the effect of single wide crack on the instability of boundary elements reinforced by plain rebars. Also it is found that although specimens with plain rebars results in single crack, the strain profile for this rebars is more uniform..

REFERENCES

[1] Lu, Y., Henri, R.S., Ma, Q.T. (2014). "Numerical modelling and testing of concrete walls with minimum vertical reinforcement." NZSEE conference.

[2] ACI 318-19 (2019). "Building code requirements for structural concrete (ACI 318-19) and commentary." American Concrete Institute, Farmington Hills, MI.

[3] Priestley, M.J.N., Seible, F., Calvi, G.M. (1996). "Seismic design and retrofit of bridges." John Wiley and Sons, NY, 686 p., doi:10.1002/9780470172858.

[4] Arteta, C.A., To, D.V., Moehle, J.P. (2014). "Experimental response of boundary elements of code-compliant reinforced concrete shear walls." Tenth U.S. National Conference on Earthquake Engineering: Frontiers of Earthquake Engineering, Anchorage, Alaska, doi:10.4231/D37H1DN29.

[5] Massone, L.M., Polanco, P., Herrera, P., (2014). "Experimental and analytical response of RC wall boundary elements." 10th U.S. National Conference on Earthquake Engineering, Anchorage, Alaska.

[6] Sritharan, S., Beyer, K., Henry, R.S., Chai, Y.H., Kowalsky, M., Bullf, D. (2014). "Understanding Poor Seismic Performance of Concrete Walls and Design Implications." Earthquake Spectra, Vol. 30, Issue 1, pp. 307-334, doi:10.1193/021713EQS036M.

[7] Hoult, R.D., Goldsworthy, H.M., Lumantana, E. (2016) . Displacement capacity of lightly reinforced rectangular concrete walls." Australian Earthquake Engineering Society 2016 Conference, Melbourne, Victoria.

[8] Lu, Y., Henry, R.S., Gultom, R., Ma, Q.T. (2017). "Cyclic testing of reinforced concrete walls with distributed minimum vertical reinforcement." ASCE Journal of Structural Engineering, Vol. 143, Issue 5, doi:10.1061/(ASCE)ST.1943-541X.0001723.

[9] NZS 3101 (2006). "Concrete structures standard (Amendment 3)." Wellington, New Zealand.

[10] Paulay, T., Priestley, M.J.N. (1992). "Seismic design of reinforced concrete and masonry building." John Wiley and Sons, 744 p., doi:10.1002/9780470172841.

[11] Rosso, A., Jimenez-Roa, L.A., Almeida, J.P., Blando, C.A., Bonett, R.L., Beyer, K. (2018). "Cyclic tensile-compressive tests on thin concrete boundary elements with a single layer of reinforcement prone to out-of-plane instability." Bulletin of Earthquake Engineering, Vol. 16, Issue 2, pp. 859-887, doi:10.1007/s10518-017-0228-1.

[12] Haro, A.G., Kowalsky, M., Chai, Y.H., Luciera, G.W. (2018). "Boundary Elements of Special Reinforced Concrete Walls Tested under Different Loading Paths." Earthquake Spectra, Vol. 34, Issue 3, pp. 1267-1288, doi:10.1193/081617EQS160M.

[13] Kawashima, K., Hosoiri, K., Shoji, G., Sakai, J. (2001). "Effects of Un-Bonding of Main Reinforcements at Plastic Hinge Region on Enhanced Ductility of Reinforced Concrete Bridge Columns." Structural and Earthquake Engineering. Proceedings of Japan Society of Civil Engineering, 689 (I-57), pp. 45-64, doi:10.2208/jscej.2001.689_45.

[14] Mashal, M., Palermo, A. (2019). "Emulative Seismic Resistant Technology for Accelerated Bridge Construction." Elsevier Journal of Soils Dynamics and Earthquake Engineering, Special Issue on Earthquake Resilient Buildings, 120, doi:10.1016/j.soildyn.2018.12.016.

[15] Nikoukalam, M. T., Sideris, P. (2016). "Experimental Performance Assessment of Nearly Full-Scale Reinforced Concrete Columns with Partially Debonded Longitudinal Reinforcement." ASCE Journal of Structural Engineering, Vol. 143, Issue 4, doi:10.1061/(ASCE)ST.1943-541X.0001708.

[16] Patel, V.J., , Van, B.C., Henry, R.S., Clifton, G.C. (2015). "Effect of reinforcing steel bond on the cracking behavior of lightly reinforced concrete members." Construction and Building Materials, Vol. 96, Issue 2, pp. 238–247, doi:10.1016/j.conbuildmat.2015.08.014.

[17] Priestley M. J. N., Park R. (1987). "Strength and ductility of concrete bridge columns under seismic loading." ACI Structural Journal, Vol. 84, Issue 1, pp. 61-76.

[18] Berry, M., Lehman D. E., Lowes L. N. (2008). "Lumped-Plasticity Models for Performance Simulation of Bridge Columns." ACI Structural Journal, Vol. 105, Issue 3, pp. 270-279.

[19] Naderpour, H., P. Fakharian. P. (2016). "A synthesis of peak picking method and wavelet packet transform for structural equation: Modal identification." KSCE Journal of Civil Engineering, Vol. 20, Issue 7, pp. 2859–2867, doi:10.1007/s12205-016-0523-4.

[20] Jahangir H., Esfahani M.R. (2012). "Structural Damage Identification Based on Modal Data and Wavelet Analysis." 3rd National Conference on Earthquake Structure, Kerman, Iran.

[21] Seyedi S.R., Keyhani A., Jahangir H. (2015). "An Energy-Based Damage Detection Algorithm Based on Modal Data. 7th International Conference on Seismology Earthquake Engineering." International Institute of Earthquake Engineering and Seismology (IIEES), pp. 335–336.

[23] Daneshvar, M.H., Gharighoran, A., Zareei, S.A., Karamodin, A. (2020). "Damage Detection of Bridge by Rayleigh-Ritz Method." Journal of Rehabilitation in Civil Engineering Vol. 8, Issue 1, pp. 149-162.

[24] Kaklauskas, G., Sokolov, A., Ramanauskas, R., Jakubovskis, R., (2019). "Reinforcement Strains in Reinforced Concrete Tensile Members Recorded by Strain Gauges and FBG Sensors: Experimental and Numerical Analysis." Sensors, Vol. 19, Issue 1, pp. 1-13, doi:10.3390/s19010200.

[25] Matsumoto, Y. (2009). "Study of the Residual Deformation Capacity of Plastically Strained." Steel, Yokohama National University, Yokohama, Kanagawa, Japan, Taylor Francis Group, London, UK.

[26] Hilson, C.W., Segura, C.L., Wallace, J.W. (2014). "Experimental study of longitudinal reinforcement buckling in reinforced concrete structural wall boundary element." Tenth U.S. National Conference on Earthquake Engineering: Frontiers of Earthquake Engineering, Anchorage, Alaska, doi:10.4231/D3CC0TT9C.

[27] Altheeb, A., Albidah, A., Lam, N.T.K., Wilson, J. (2013). "The development of strain penetration in lightly reinforced concrete shear walls." Australian Earthquake Engineering Society 2013, Hobart, Tasmania.